

Deconversion of Power-Law Noise to White Noise Through Direct and Indirect Model Inversion

Naleli Jubert Matjelo¹

¹National University of Lesotho, Department of Physics and Electronics, P. O. Roma 180, Lesotho

Abstract:- This paper gives an account of how power-law noise power spectral density can be deconverted to white noise power spectral density. The analysis is carried out both in the frequency domain using transfer function models as well as in the time domain using state-space models whereby a linear time-invariant model being used to generate approximate power-law noise from white noise after which this model is inverted directly and indirectly. Both direct (open-loop) model inversion and indirect (closed-loop) model inversion are simulated and discussed. It is through these simulations that the indirect model inversion performance is shown to increases with increasing feedback control gain.

Keywords:- State-Space Model, Power-Law Noise, Model Inversion, Barnes-Jarvis Model, Feedback Control.

INTRODUCTION

Understanding the type of noise that underlies the data allows one to be able to devise appropriate means of filtering the particular noise that seems to be dominant. Power-law noise is a major contributor to the overall noise in many systems, including electronic resonators and oscillators [1], [2], [3], [4], quantum systems [5], [6], and sensors [7]. Most resonators and oscillators are affected by noise whose power spectral density $S_y(f)$ obeys the power-law as shown below,

$$S_y(f) \propto f^\lambda \quad (1)$$

where f is the noise frequency in Hz. The exponent λ takes on different values depending on the kind of power-law noise involved. Some examples include white noise ($\lambda = 0$), flicker noise ($\lambda = -1$), random walk noise ($\lambda = -2$), and random run noise ($\lambda = -4$) [8]. In this paper, we present two ways of deconverting power-law noise into white noise through direct inversion as well as through feedback inversion of the power-law noise model. This means we begin by adopting a model generating some power-law noise and take its reciprocal in one case while in the other case we apply feedback control to convert the underlying power-law noise into white noise. The main reason for choosing white noise as a target or setpoint is because a lot of filtering algorithms work very well with white noise thus being able to deconvert any noise type into white noise would allow various tools optimized for white noise to be utilized for any noise. The model that we adopt for power-law noise generation is the model by Barnes and Jarvis, which is formed by a cascade of first-order filters [9].

The rest of this paper is organized as follows. Section II presents the Barnes-Jarvis model as a cascade of first-order filters in the frequency domain which gets converted to a state-space model. Section III presents the two ways of inverting the Barnes-Jarvis model with the aim of deconverting power-law noise to white noise. The first model inversion approach takes a direct reciprocal of the Barnes-Jarvis transfer function while the second approach considers the feedback control scheme as a way of model inversion. Section IV presents and discusses the simulation results obtained from the Barnes-Jarvis model and its two inversion approaches. Section V concludes this paper with some major aspects of this work and some remarks and possible future work.

BARNES-JARVIS MODEL

2.1 Frequency Domain Model

In this section, we consider a cascade model from the previous section and show its Bode diagram and power spectral density, which falls approximately as $1/f$ over a frequency interval dictated by the choice of τ and β^m . The transfer function $G(s)$ for this cascade model is shown below,

$$G(s) = \prod_{i=1}^{m-1} \frac{\tau s + \beta^i}{\alpha \tau s + \beta^i} \quad (2)$$

The equation $\beta \alpha^{\frac{2}{\lambda}} = 1$ fixes the relationship between α and β where λ is the slope characterizing the power spectral density of the power-law noise. Theoretically, this slope can be estimated well in the frequency range $\left[\frac{\beta^0}{2\pi\tau}, \frac{\beta^m}{2\pi\tau}\right]$.

2.2 State Space Model

The transfer function model in the previous section can be converted to a continuous-time state-space model and discretized. The corresponding discrete-time state-space model has the following form,

$$\mathbf{z}_{k+1} = \mathbf{A}\mathbf{z}_k + \mathbf{B}u_k \quad (3)$$

$$y_k = \mathbf{C}^T \mathbf{z}_k + \mathbf{D}u_k \quad (4)$$

where k represents the k^{th} time instance at time $t = kT$ for some sampling period T and the discrete-time matrices are given by,

$$\mathbf{A} = e^{\mathbf{A}_c T} \quad (5)$$

$$\mathbf{B} = \mathbf{A}_c^{-1}(e^{\mathbf{A}_c T} - \mathbf{I})\mathbf{B}_c \quad (6)$$

The continuous-time matrices \mathbf{A}_c , \mathbf{B}_c , \mathbf{C} and \mathbf{D} for model size $m = 4$ are given by,

$$\mathbf{A}_c = \begin{bmatrix} -\beta^0 & 0 & 0 & 0 \\ \frac{(\alpha-1)\beta^0}{\alpha\tau} & \frac{-\beta^1}{\alpha\tau} & 0 & 0 \\ \frac{(\alpha-1)\beta^0}{\alpha^2\tau} & \frac{(\alpha-1)\beta^1}{\alpha^2\tau} & \frac{-\beta^2}{\alpha\tau} & 0 \\ \frac{(\alpha-1)\beta^0}{\alpha^3\tau} & \frac{(\alpha-1)\beta^1}{\alpha^3\tau} & \frac{(\alpha-1)\beta^2}{\alpha^2\tau} & \frac{-\beta^3}{\alpha\tau} \end{bmatrix} \quad (7)$$

$$\mathbf{B}_c^T = \begin{bmatrix} \frac{1}{\alpha^1\tau} & \frac{1}{\alpha^2\tau} & \frac{1}{\alpha^3\tau} & \frac{1}{\alpha^4\tau} \end{bmatrix} \quad (8)$$

$$\mathbf{C}^T = (\alpha - 1) \begin{bmatrix} \beta^0 & \beta^1 & \beta^2 & \beta^3 \\ \alpha^4 & \alpha^3 & \alpha^2 & \alpha^1 \end{bmatrix} \quad (9)$$

$$\mathbf{D} = \begin{bmatrix} \frac{1}{\alpha^4} \end{bmatrix} \quad (10)$$

The next section gives an account of converting power-law noise back to white noise through model inversion mechanisms.

BARNES-JARVIS MODEL INVERSION

3.1 Direct Inversion Transfer Function Model

The direct model inversion is built on the idea of reversing the signal flow of the open-loop system presented in equation (2). That is, given u_k (or $u(t)$) and y_k (or $y(t)$) to be white noise input and power-law noise output respectively as per Barnes-Jarvis model $G(s)$ outlined in the previous section, we now reverse the signal flow and invert the model as follows,

$$U(s) = \frac{1}{G(s)} Y(s) \quad (11)$$

with $U(s)$ and $Y(s)$ as Laplace transforms of $u(t)$ and $y(t)$ respectively. This means that now we have power-law noise, $y(t)$ as input to our inverted model $G(s)$ and white noise $u(t)$ as output. This direct way of inversion is seldom done in control theory due to it being prone to instabilities arising from possible non-minimum phase zeros as well as it lacking the ability to reject disturbances from outside. In the case of the Barnes-Jarvis model, there are no non-minimum phase zeros since the numerator for each i^{th} cascade leads to a negative zero, (i.e. $s = \tau^{-1}\beta^i$) hence the inverted model is both causal and stable. However, disturbance-rejection is not enhanced as shown next.

Consider input disturbance $i(t)$ and output disturbance $o(t)$ which are additively coupled to the inverted model as shown in Fig. 1 below.

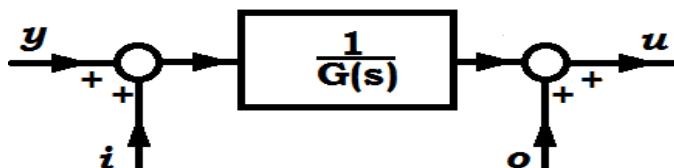


Fig. 1. Inverted Barnes-Jarvis model with input and output disturbances.

The transfer function relating the input disturbance $i(t)$ to the output $u(t)$ is given by,

$$\frac{U(s)}{I(s)} = \frac{1}{G(s)} \quad (12)$$

This means the input disturbance $i(t)$ is on equal footing with our input $y(t)$ hence the setup offers no input disturbance rejection or suppression relative to the desired input $y(t)$. Looking at the output disturbance $o(t)$ we can see that it proceeds to the output unattenuated at all, hence there is no output disturbance rejection either. The next section state-space representation of this direct inversion model.

3.2 Direct Inversion State Space Model

The transfer function of the inversion model can be converted into a continuous-time state-space model and discretized. The corresponding discrete-time state-space model has the following form,

$$\mathbf{z}_{k+1} = \mathbf{E}\mathbf{z}_k + \mathbf{F}u_k \quad (13)$$

$$u_k = \mathbf{M}^T \mathbf{z}_k + \mathbf{N}u_k \quad (14)$$

whereas before, k represents the k^{th} time instance at time $t = kT$ for some sampling period T and the discrete-time matrices are obtained using the same procedure as in the case of equation (5 - 6). The rest of the variables are y_k as the input flicker noise, u_k as the estimated output white noise, \mathbf{z}_k as the state vector and the continuous-time matrices \mathbf{E}_c , \mathbf{F}_c , \mathbf{M} and \mathbf{N} for model size $m = 4$ are given by,

$$\mathbf{E}_c = \begin{bmatrix} -\beta^0 & 0 & 0 & 0 \\ \frac{\tau}{\beta^1} & \frac{(1-\alpha)\alpha^0\beta^0}{\tau} & 0 & 0 \\ -\beta^2 & \frac{(1-\alpha)\alpha^0\beta^1}{\tau} & \frac{(1-\alpha)\alpha^1\beta^0}{\tau} & 0 \\ \frac{\tau}{\beta^3} & \frac{(1-\alpha)\alpha^0\beta^2}{\tau} & \frac{(1-\alpha)\alpha^1\beta^1}{\tau} & \frac{(1-\alpha)\alpha^2\beta^0}{\tau} \end{bmatrix} \quad (15)$$

$$\mathbf{F}_c^T = \begin{bmatrix} \frac{\tau}{\alpha^0} & \frac{\tau}{\alpha^1} & \frac{\tau}{\alpha^2} & \frac{\tau}{\alpha^3} \end{bmatrix} \quad (16)$$

$$\mathbf{M}^T = (1 - \alpha)[\alpha^3\beta^0 \quad \alpha^2\beta^1 \quad \alpha^1\beta^2 \quad \alpha^0\beta^3] \quad (17)$$

$$\mathbf{N} = [\alpha^4] \quad (18)$$

The next section considers a feedback control loop approach for model inversion.

3.1 Indirect Inversion Transfer Function Model

Consider a feedback control loop applied to Barnes-Jarvis model as shown in Fig. 2 below.

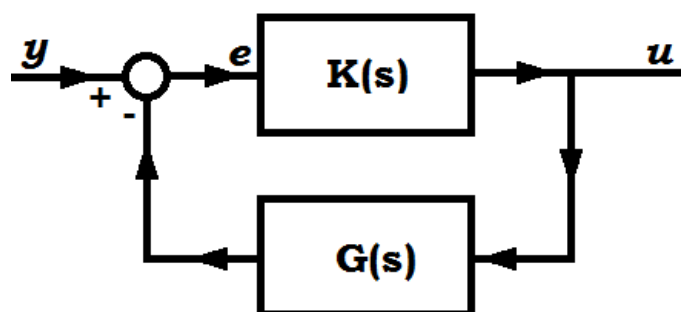


Fig. 2. Feedback control loop as an indirect inversion approach.

The transfer function relating our power-law noise input $y(t)$ to the white noise output $u(t)$ is given as,

$$\frac{U(s)}{Y(s)} = \frac{K(s)}{1+K(s)G(s)} \quad (19)$$

with $K(s)$ as the controller. Notice that for a large value of control gain $K(s)$ the transfer function approaches the direct inversion model presented in the previous section. Hence by tuning the control gain one can get the same results as those of the direct inversion model outlined above.

3.1 Indirect Inversion State Space Model

In this section, we consider full state feedback (as opposed to output feedback) and we proceed to close the loop by making the following setting on the open-loop Barnes-Jarvis model in equations (3 - 4)

$$u(t) = K(y(t) - z(t)) \quad (20)$$

with $y(t) = Ky(t)$ from the input power-law noise and $u(t)$ being the white noise resulting from the indirect inversion of $y(t)$. This leads to the following discrete-time state-space model,

$$z_{k+1} = Pz_k + Qu_k \quad (21)$$

$$u_k = -Kz_k + y_k \quad (22)$$

with P and Q obtained in the same way as the discrete-time transition and input matrices in equation (5 - 6). The next section presents flicker noise simulation results for the Barnes-Jarvis model and the two inversion approaches.

4. SIMULATION RESULTS

4.1 Approximating 1/f Noise With Barnes-Jarvis Model

Fig. 3 below shows the power spectral density plot of a flicker noise data (as reference) and the above Barnes-Jarvis discrete-time state-space model simulation output with $T = 12\text{ ms}$, $\lambda = -1$, $\tau = 3\text{ s}$, $\alpha = 3$ and $\beta = 9$.

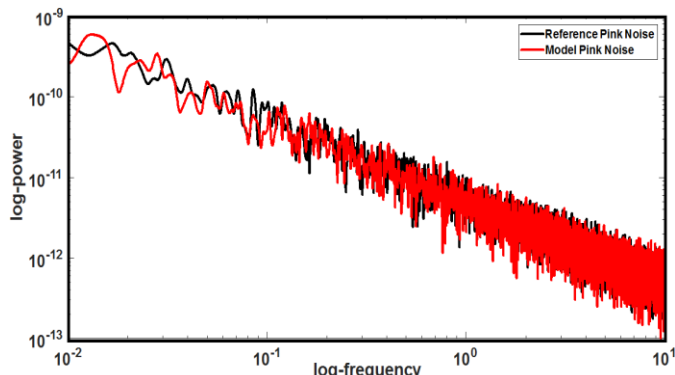


Fig. 3. Barnes-Jarvis discrete-time state-space model simulation.

In Fig. 3 above it can be seen that the Barnes-Jarvis model is approximating the flicker noise reasonably well for the first two decades. Theoretically, it is expected that the model will deviate from the expected flicker/pink noise profile towards the edges of the following frequency range, $\left[\frac{\beta^0}{2\pi\tau}, \frac{\beta^m}{2\pi\tau}\right] = [53\text{ mHz} \quad 348\text{ Hz}]$.

4.1 Low Feedback Control Gain

Fig. 4 below shows the results of directly and indirectly inverting the Barnes-Jarvis model under similar settings (i.e. with $T = 12\text{ ms}$, $\lambda = -1$, $\tau = 3\text{ s}$, $\alpha = 3$ and $\beta = 9$) presented in the previous section. In this case, the control gain matrix for indirect inversion is $K = [2 \quad 1 \quad 6 \quad 5]$.

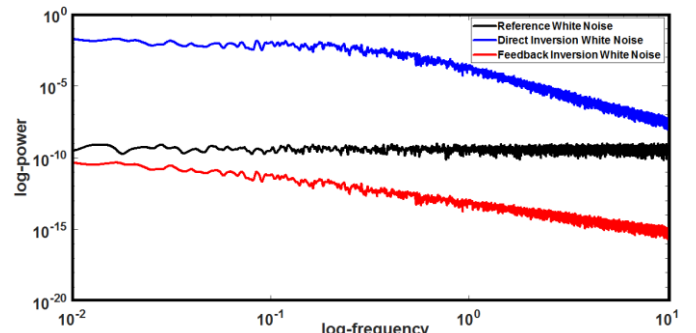


Fig. 4. Power spectral densities for both direct and indirect model inversion of the Barnes-Jarvis model under low feedback control gain.

It can be seen that the direct inversion approach can convert the flicker noise to white noise better in low frequencies compared to higher frequencies. The indirect inversion approach seems to be unable to perform well across the shown frequency spectrum. The next section presents the same simulation with the control gain increased by a factor of 100.

4.1 High Feedback Control Gain

Fig. 5 below shows the simulation results under similar settings as in the previous section with the only exception that here the control gain matrix is increased to $K = [200 \quad 100 \quad 600 \quad 500]$.

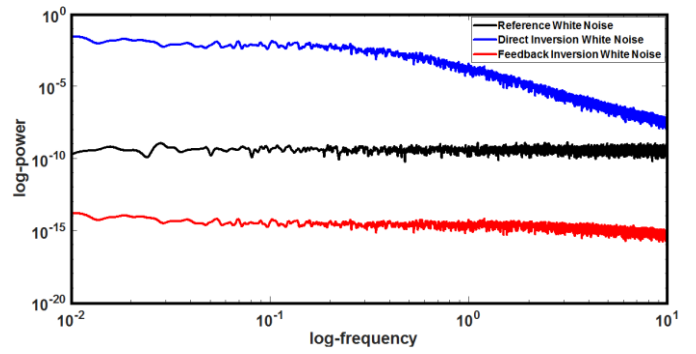


Fig. 5. Power spectral densities for both direct and indirect model inversion of the Barnes-Jarvis model under high feedback control gain.

While the direct inversion approach remains the same, the indirect inversion approach seems to be performing well over a much wider frequency spectrum than the direct inversion approach. These inversion approaches show that it is possible to deconvert power-law noise to white noise which can then be processed further using well-known tools. In the

case whereby the signal of interest is expected to be near zero (i.e. laser detuning from some atomic transition), the signal fluctuations will be mostly due to power-law noise which can be deconverted to white noise can be filtered out using common white noise filtering techniques.

CONCLUSIONS

In this paper, we presented two ways of inverting the power-law noise model such that the resulting inverted models can decompose the input power-law noise into white noise which is easier to filter. Barnes-Jarvis model was set up to adaptively track and estimate the reference flicker noise in the frequency band [53 mHz 348 Hz]. The two inversion models successfully inverted part of the reference flicker noise spectrum back into white noise while the other part of the spectrum was not well-converted back to white noise. The indirect inversion, using feedback control with high gain, appeared to be able to convert a wider spectrum of flicker noise than the direct inversion approach. However, under low gain setting the indirect inversion was performing poorly across the whole spectrum. The indirect inversion approach is much more robust and easier to implement than the direct inversion approach especially in cases whereby the underlying noise is a weighted aggregation of different power-law noise types, which is more likely to be the case in practice.

REFERENCES

- [1]. Kasdin N. J. and Walter T. Discrete simulation of power-law noise (for oscillator stability evaluation). In Proceedings of the 1992 IEEE Frequency Control Symposium, pages 274–283, 1992.
- [2]. Chen X. Peng C. Huan H. Nian F. and Yang B. Measuring the Power Law Phase Noise of an RF Oscillator with a Novel Indirect Quantitative Scheme. *Electronics*, 8, 767:1–9, 2013.
- [3]. Chorti A. and Brookes M. A Spectral Model for RF Oscillators With Power-Law Phase Noise. *IEEE Transactions On Circuits and Systems-I: Regular Papers*, 53, 9:1989 – 1999, 2006.
- [4]. Macucci M. and Marconcini P. Theoretical Comparison between the Flicker Noise Behavior of Graphene and Ordinary Semiconductors. *Journal of Sensors*, 2020:11, 2020.
- [5]. Oliver W. D. Ball H. and Biercuk M. J. The role of master clock stability in quantum information processing. *njp Quantum Information*, 2, 16033:1– 8, 2016.
- [6]. arxiv:1304.7925 [cond-mat.mes-hall].
- [7]. Falci G. D'Arrigo A. and Paladino E. Quantum Sensing 1/f Noise via Pulsed Control of a Two-Qubit Gate. In Proceedings 2019012029, pages 1–8, 2019, 12, 29.
- [8]. Greenhall C. A. An approach to power-law phase-noise models through generalized functions. *Metrologia*, 47:605 – 615, 2010.
- [9]. Jarvis S. Barnes J. Efficient numerical and analog modeling of flicker noise processes. National Bureau of Standards Technical Note 604, 1971.